ChemComm
Chemical Communications

Accepted Manuscript

This article can be cited before page numbers have been issued, to do this please use: L. Xia, M. Li, H. Wang, R. Yuan and Y. Chai, *Chem. Commun.*, 2019, DOI: 10.1039/C9CC04899E.

ROYAL SOCIETY OF CHEMISTRY

rsc.li/chemcomm

Journal Name

View Article Online
DOI: 10.1039/C9CC04899E

COMMUNICATION

A Novel "Signal On" Photoelectrochemical Strategy Based on Dual Functional Hemin for MicroRNA Assay

Received 00th January 20xx,
Accepted 00th January 20xx

DOI: 10.1039/x0xx00000x

www.rsc.org/

Ling-Ying Xia, Meng-Jie Li, Hai-Jun Wang, Ruo Yuan* and Ya-Qin Chai*

In this work, a novel "signal on" photoelectrochemistry (PEC) biosensor was constructed by dual functional hemin as signal quencher and electronic mediator for ultrasensitive target microRNA-141 assay with the assistance of T7 exonuclease (Exo)-initiated target amplification technology.

Photoelectrochemistry (PEC) assay as a newly emerged analytical method has attracted growing attention owing to its exquisite merits of low background, high sensitivity and outstanding stability.[1-7] Recently, numerous "signal off" PEC sensors were constructed based on different types of signal quenching strategies including resonance energy transfer,[8] steric hindrance[9] and electronic competition[10]. For instance, Chen's group has fabricated a "signal off" PEC biosensor based on energy transfer between gold nanoparticles (Au NPs) and semiconducting polymer dots.[11] Our group has proposed an ultrasensitive PEC biosensor using SiO_2 as the signal quencher of PTB7-Th due to the steric hindrance of SiO_2.[12] Although greatly improved analytical performance was obtained in the above works, these "signal off" PEC strategies suffered from an unidirectional quenching effect, which would lead to narrow detection range and limited sensitivity for PEC assay. Therefore, we hypothesis that integrating the quenching effect and signal enhancement into one strategy by a dual functional material may significantly broaden the detection range and simultaneously improve the sensitivity of the PEC assay.

Iron-(III) protoporphyrin IX chloride (hemin) as an iron(III) porphyrin complex has been widely applied in electrocatalysis and bioanalysis because of its exquisite properties of low toxicity, peroxidase-like activity and excellent electronic acceptability.[13-18] Xie's group has reported a biosensor based on the quenching effect of hemin to Ag nanocluster.[19] In Yang's work, a "signal off" biosensor was constructed using hemin as the signal quencher for the fluorophore.[20] Therefore, hemin could be employed as a potential PEC signal quencher due to the electronic acceptability of Fe^{3+} in hemin. Besides, a mutual conversion from Fe^{3+} to Fe^{2+} in hemin could be achievable by the transformation of electrons or holes,[21-24] which demonstrated hemin is highly promising to be used as a shuttle redox mediator in Z-scheme structure.[25-27] Moreover, hemin possesses a rational redox potential to accept electrons from $MTiO_2$.[28] In view of those advantages, hemin could not only be implemented as an efficient signal quencher to obtain extremely low initial photocurrent and broad detection range, but also act as a shuttle redox mediator in the Z scheme structure to achieve a significantly enhanced ultimate photocurrent, which broke the unidirectional quenching effect of traditional PEC signal quencher. Accordingly, it is expected to construct a novel "signal on" PEC biosensor based on the dual functional hemin for the ultrasensitive detection of microRNA.

In this work, a novel "signal on" PEC biosensor was established based on the dual functional hemin for ultrasensitive microRNA-141 detection with the assistance of T7 Exonuclease (Exo)-initiated target amplification technology. As depicted in Scheme l, meso-porous TiO_2-hemin ($MTiO_2$-hemin) was modified on the surface of bare glassy carbon electrode (GCE) and served as the substrate of the PEC biosensor to provide a low initial photocurrent signal owing to the quenching effect of hemin to $MTiO_2$. Followed by the deposition of Au NPs, duplex of H1/S1 was incubated on the resultant electrode by Au-N bond. Next, hexanethiol (HT), used as blocking agent, was incubated on the modified electrode. After the addition of target (microRNA-141), H1 was displaced by microRNA-141 and a DNA-RNA duplex (S1/microRNA-141) was generated. In the presence of T7 Exo, S1 was cleaved to shattered nucleotides and the target was released for reusing. Through the T7 Exo-initiated target amplification technology, a lot of single strand H1 were released on the electrode surface. With the addition of H2-CdS QDs, the duplex of H1/H2 was produced and CdS QDs closed to the surface of electrode. With the introduction of CdS QDs, the Z-scheme structure of $MTiO_2$-hemin-CdS QD was established, in which hemin as an electron mediator, and a significantly enhanced photocurrent signal was obtained, thereby realizing highly sensitive detection of microRNA-141. This work featured firstly a novel dual functional material for constructing ultrasensitive PEC

Key Laboratory of Luminescence and Real-Time Analytical Chemistry (Southwest University), Ministry of Education, College of Chemistry and Chemical Engineering, Southwest University, Chongqing 400715, P. R. China.
E-mail: yuanruo@swu.edu.cn, yaqinchai@swu.edu.cn;
Fax: +86-23-68253172; Tel: +86-23-68252277
Electronic Supplementary Information (ESI) available: Experimental Section; PEC Characterization of the Proposed Biosensor; Electrochemical Characterization of the Proposed Biosensor, Optimization of the Concentration of Substrate, PAGE Analysis. See DOI: 10.1039/x0xx00000x

biosensor, which opened a new way for detection of biomarkers.

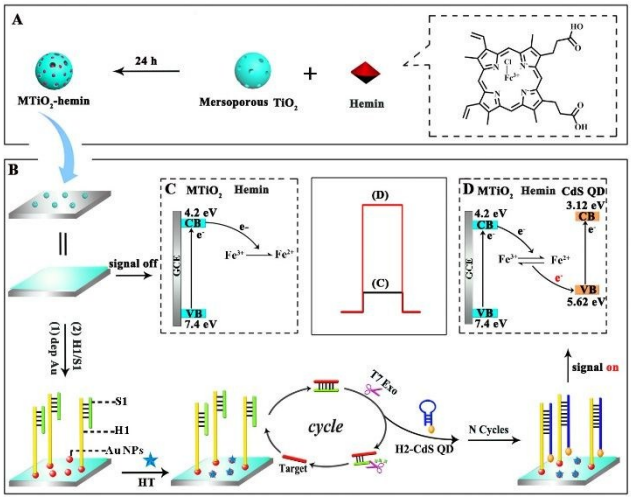

Scheme 1. Schematic illustration of (A) the Preparation Process of $MTiO_2$-Hemin, (B) the Fabrication Process of the PEC Biosensor; (C) the Electron Transfer in $MTiO_2$-Hemin, and (D) the Electron Transfer in the Z Scheme Structure of $MTiO_2$-Hemin-CdS QDs.

The morphologies of synthesized CdS QDs and $MTiO_2$ were characterized by transmission electron microscope (TEM) and scanning electron microscope (SEM), respectively. As shown in Figure 1A and 1B, CdS QDs were subjected to TEM. Figure 1A showed the TEM image of CdS QDs and Figure 1B showed the high resolution TEM (HRTEM) image of CdS QDs, which displayed the size of CdS QDs was about 5 nm. Meanwhile, obvious lattice arrangement could be observed in the HRTEM image. In addition, $MTiO_2$ particles were characterized by scanning electron microscope (SEM). As can be seen in Figure 1C, numerous $MTiO_2$ particles could be observed. In the view of high resolution, the size of $MTiO_2$ particle was about 840 nm with a globular in shape, which was showed in Figure 1D. From a higher resolution than that of Figure 1D, Figure 1E showed that $MTiO_2$ particle was composed with 10 nm of nanocrystals. From the above results, we could infer that the CdS QDs and $MTiO_2$ were successfully synthesized.

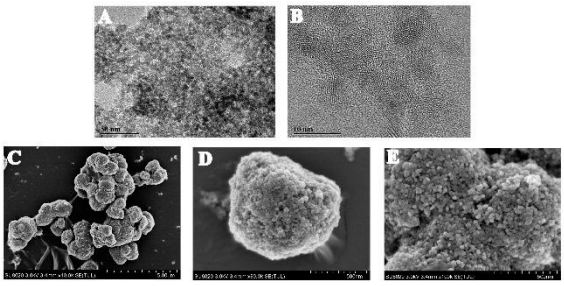

Figure 1. TEM (A) and HRTEM (B) of the prepared CdS QDs; The SEM images of the $MTiO_2$ particles (C, D and E) under different resolutions.

Ultraviolet-visible (UV-vis) spectra was applied to investigate the linking of hemin to $MTiO_2$ surface. Figure 2A showed the UV-vis spectra of $MTiO_2$ particles, in which a wide absorption peak in the range of 200 nm ~ 400 nm was obtained while no obvious absorption peak could be found in the range of 400 ~ 800 nm. In Figure 2B, the characterized absorption peaks of hemin could be observed at 389 nm and 594 nm. When hemin was linked on the surface of $MTiO_2$ particles, the absorption peaks changed evidently. Compared with Figure 2B, the $MTiO_2$-hemin spectrum (Figure 2C) contained the characteristic absorption peak of $MTiO_2$ and hemin with a red shift from 389 nm to 398 nm originated from the generation of covalent bonds between $MTiO_2$ and hemin, which was consistent with the reported literature.[29] The result illustrated the successful linking of hemin to the surface of $MTiO_2$ particles.

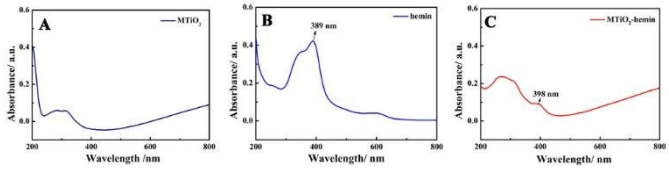

Figure 2. UV-vis adsorption spectra of (A) $MTiO_2$ particles, (B) hemin and (C) $MTiO_2$-hemin.

To investigate the process of "signal on" in this strategy, different PEC responses were measured by immobilizing different materials on the surface of GCE. In Figure 3A, after modifying pure $MTiO_2$ on the bare electrode, about 328 nA of photocurrent could be obtained. However, a significantly reduced PEC signal (45 nA) was obtained by incubating $MTiO_2$-hemin on the bare GCE due to the signal quenching effect of hemin to $MTiO_2$ (Figure 3B). Compared to the PEC signal of $MTiO_2$, the PEC signal of $MTiO_2$-hemin reduced by 87%. Furthermore, an obviously increased PEC signal of 874 nA was generated by introducing CdS QDs to form Z-scheme structure of $MTiO_2$-hemin- CdS QDs (Figure 3C). The results demonstrated that dual functional hemin was successfully used as the signal quencher of $MTiO_2$ to efficiently quench the PEC signal of $MTiO_2$ and as the electron mediator in the Z-scheme structure of $MTiO_2$-hemin-CdS QDs to improve the ultimate PEC signal.

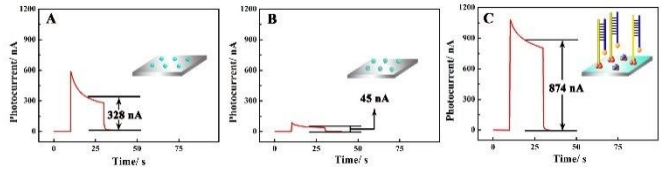

Figure 3. PEC responses for different materials: (A) $MTiO_2$/GCE; (B) $MTiO_2$-hemin/GCE; (C) H2-CdS QDs/T7 Exo/microRNA-141/HT/H1/S1/Au NPs/$MTiO_2$-hemin/GCE.

The process of electron transformation was combined of "signal-off" and "signal-on". As shown in Figure 4A, the excited electrons in $MTiO_2$ transferred from the valance band (VB) to the conductive band (CB) of $MTiO_2$. With the existence of hemin, the electron could migrate from the CB of $MTiO_2$ to Fe^{3+} in hemin because of the excellent electronic acceptability of Fe^{3+}. As a result, the photocurrent was obviously quenched and "signal-off" was achieved, which could effectively sharply reduce the background signal of the biosensor. The "signal-on" was achieved by introducing CdS QDs into closing proximity to the $MTiO_2$-hemin. As shown in Figure 4B, a conversion between Fe^{2+} and Fe^{3+} was facile and the electrons located in hemin had a strong tendency to transfer to the VB of CdS QDs due to electrostatic attraction. Then, numerous electrons on the VB of CdS QDs could jump to the CB of CdS QDs. Through such a

process, a significantly enhanced photocurrent could be expected on the basis of the accelerated electron-hole pairs separation speed and the reduced electron-hole pairs recombination rate, which increased the ultimate signal in PEC assay.

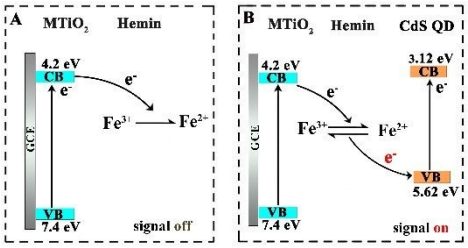

Figure 4. Electron transferred scheme of (A) initial signal and (B) ultimate signal in the proposed PEC biosensor.

To estimate the performance of the proposed PEC platform, microRNA-141 was used as the target model with various concentrations. As shown in Figure 5, the photocurrent was increased with the increase of the concentration of microRNA-141 in the range of 0.25 fM to 2.5 nM, which indicated that the immobilization amount of CdS QDs was highly dependent on the concentration of target. The regression equation is $I = 119.7 \lg c + 132.8$ ($R = 0.9936$) (I, c, and R are the PEC signals, microRNA-141 concentrations, and correlation coefficient, respectively). Also, a low limit of detection (LOD) of 139 aM was obtained. Furthermore, the linear range and the LOD of our proposed PEC biosensor for microRNA-141 were comparable to those of previous strategies, which were showed in Table S2. The results demonstrated that the proposed biosensor possessed excellent sensitivity for the detection of microRNA-141.

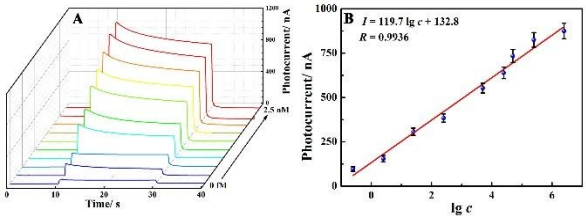

Figure 5. (A) PEC response of the biosensor with various concentrations of target microRNA-141 (0 fM, 0.25 fM, 2.5 fM, 25 fM, 0.25 pM, 2.5 pM, 25 pM, 50 pM, 0.25 nM, 2.5 nM); (B) Derived calibration curve of PEC response vs the logarithm of target microRNA-141 concentration (0.25 fM, 2.5 fM, 25 fM, 0.25 pM, 2.5 pM, 25 pM, 50 pM, 0.25 nM, 2.5 nM).

To study the specificity of the proposed platform for microRNA-141 detection, thrombin (TB), microRNA-21, microRNA-155 and microRNA-182-5p were employed as the references. As shown in Figure 6A, a high photocurrent of the biosensor was obtained when microRNA-141 (25 pM) was incubated while low photocurrent signals were found when the electrodes were incubated with thrombin (0.25 nM), microRNA-21 (0.25 nM), microRNA-155 (0.25 nM) and microRNA-182-5p (0.25 nM), which were the same with that of the blank sample. All the results illustrated that the biosensor possessed excellent selectivity. Meanwhile, stability of the biosensor was estimated by continuously scanning 8 cycles of the proposed biosensor incubated with 2.5 pM microRNA-141. Figure 6B showed admirable stability of the proposed biosensor with relative standard deviation (RSD) of 1.43%.

For the purpose of verifying the feasibility of the proposed PEC biosensor for detection of microRNA-141, two different cancer cell lines including MB231 and Hela were employed as the actual samples. As can be seen in Figure 7, with the increasing cancer cell number from 10 to 1000, the PEC signal was increased. Meanwhile, the PEC signal of MB231 was clearly higher than that of Hela. These results indicated that microRNA-141 was high expressed in MB231 cells, while low expressed in Hela cells, which was consistent with reported literatures.[30,31] Thus, the proposed PEC biosensor showed excellent performance for clinical applications in early diagnosis of cancers.

View Article Online
DOI: 10.1039/C9CC04809E

Figure 6. (A) Specificity of the PEC biosensor toward target (25 pM), blank and different interferences: 0.25 nM of TB, 0.25 nM of microRNA-21, 0.25 nM of microRNA-155, 0.25 nM of microRNA-182-5p; (B) Stability of the prepared PEC biosensor.

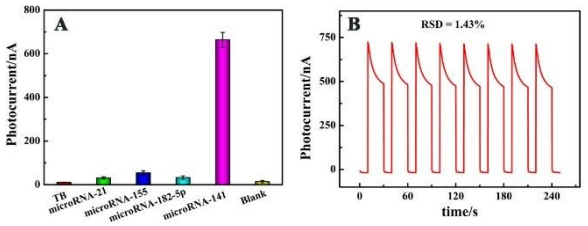

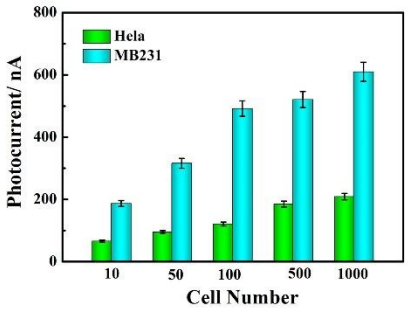

Figure 7. PEC signal of the prepared PEC biosensor from Hela and MB231 cells under different cell numbers.

In summary, a novel "signal on" PEC biosensor was constructed based on hemin as signal quencher and electronic mediator for the ultrasensitive detection of microRNA-141 with the assistance of T7 Exo-initiated target recycle amplification technology. The substrate $MTiO_2$-hemin provided an extremely low initial signal owing to the obvious quenching effect of hemin to $MTiO_2$ with a quenching efficiency of 87%. Through a T7 Exo-initiated target recycle amplification strategy, a little of target was transduced to numerous H1 probe, which further hybridized with H2 labeled CdS QDs to capture CdS QDs on the electrode surface. Moreover, the introduction of Z-scheme system ($MTiO_2$-hemin-CdS QDs) could further improve the sensitivity of the biosensor because hemin was employed as a redox shuttle mediator and conducive to obtain enhanced ultimate signal. As expected, hemin not only acted as a signal quencher of $MTiO_2$ also acted as an electronic mediator in the Z scheme system of $MTiO_2$-hemin-CdS QDs. The prepared PEC assay showed wide detection range and superior sensitivity for the analysis of microRNA. Meanwhile, this proposed strategy paved

a new prospect for the detection of biomarkers and initial diagnosis of diseases.

Acknowledgement

The authors thank the China National Natural Science Foundation (NNSF) of China (Grants 21575116, 21675129 and 21775124), and the Fundamental Research Funds for the Central Universities (Grants XDJK2018AA003) for financial assistance.

Conflicts of interest

There are no conflicts to declare.

Notes and references

1. Y. F. Tang, X. Q. Liu, H. J. Zheng, L. W. Yang, L. L. Li, S. Zhang, Y. M. Zhou, S. Alwarappan, *Nanoscale*, 2019, **11**, 9115-9124.
2. T. Hou, N. N. Xu, W. X. Wang, L. Ge, F. Li, *Anal. Chem.* 2018, **90**, 9591-9597.
3. H. H. Huo, Z. D. Xu, T. Zhang, C. L. Xu, *J. Mater. Chem. A*, 2015, **3**, 5882-5888.
4. N. Zhang, Y. F. Ruan, L. B. Zhang, W. W. Zhao, J. J. Xu, H. Y. Chen, *Anal. Chem*. 2018, **90**, 2341-2347.
5. G. M. Wen, H. X. Ju, *Anal. Chem.* 2016, **88**, 8339-8345.
6. L. X. Meng, Y. M. Li, R. Y. Yang, X. H. Zhang, C. C. Du, J. H. Chen, *Chem. Commun.*, 2019, **55**, 2182-2185.
7. C. Ye, M. Q. Wang, L. J. Li, H. Q. Luo, N. B. Li, *Nanoscale*, 2017, **9**, 7526-7532.
8. N. Zhang, X. M. Shi, H. Q. Guo, X. Z. Zhao, W. W. Zhao, J. J. Xu, H. Y. Chen, *Anal. Chem.* 2018, **90**, 11892-11898.
9. G. C. Fan, L. Han, H. Zhu, J. R. Zhang, J. J. Zhu, *Anal. Chem.* 2014, **86**, 12398-12405.
10. Q. K. Kong, K. Cui, L. N. Zhang, Y. H. Wang, J. L. Sun, S. G. Ge, Y. Zhang, J. H. Yu, *Anal. Chem.* 2018, **90**, 11297-11304.
11. X. M. Shi, L. P. Mei, Q. Wang, W. W. Zhao, J. J. Xu, H. Y. Chen, *Anal. Chem.* 2018, **90**, 4277-4281.
12. Y. N. Zheng, W. B. Liang, C. Y. Xiong, Y. L. Yuan, Y. Q. Chai, R. Yuan, *Anal. Chem.* 2016, **88**, 8698-8705.
13. Y. R. Li, Y. Y. Chang, R. Yuan, Y. Q. Chai, *ACS Appl. Mater. Interfaces* 2018, **10**, 25213-25218.
14. X. Q. Liu, R. Freeman, E. Golub, I. Willner, *ACS Nano* 2011, **5**, 7648-7655.
15. S. Wang, J. Sun, J. H. Zhao, S. S. Lu, X. R. Yang, *Anal. Chem.* 2018, **90**, 3437-3442.
16. Y. H. Guo, J. L. Chen, M. P. Cheng, D. Monchaud, J. Zhou, H. X. Ju, *Angew. Chem.* 2017, **129**, 16863-16867.
17. R. Y. Yang, K. Zou, X. H. Zhang, C. C. Du, J. H. Chen, *Biosen. Bioelectron.* 2019, **132**, 55-61.
18. Y. Li, F. T. Chen, Z. Z. Luan, X. R. Zhang, *Biosen. Bioelectron.* 2018, **119**, 63-69.
19. K. Zhang, K. Wang, X. Zhu, Y. Gao, M. H. Xie, *Chem. Commun.*, 2014, **50**, 14221-14224.
20. S. Wang, J. Sun, J. H. Zhao, S. S. Lu, X. R. Yang, *Anal. Chem.* 2018, **90**, 3437-3442.
21. A. Hirano, M. Wada, T. Tanaka, H. Kataura, *ACS Nano* 2019, **13**, 1805-1816.
22. H. J. Zhang, Y. M. Kou, J. B. Li, L. Chen, Z. Mao, X. X. Han, B. Zhao, Y. Ozaki, *Anal. Chem.* 2019, **91**, 1213-1216.
23. L. B. Zhang, J. B. Zhu, S. J. Guo, T. Li, J. Li, E. K. Wang, *J. Am. Chem. Soc.* 2013, **135**, 2403-2406.
24. S. O. Obare, T. Ito, M. H. Balfour, G. J. Meyer, *Nano Lett.* 2003, **3**, 1151-1153.
25. J. X. Low, C. J. Jiang, B. Cheng, S. Wageh, A. A. Al-Ghamdi, J. G. Yu, *Small Methods* 2017, **1**, 1700080-1700101.
26. H. Kato, Y. Sasaki, N. Shirakuraa, A. Kudo, *J. Mater. Chem. A,* 2013, **1**, 12327-12333.
27. W. G. Tu, Y. Zhou, S. C. Feng, Q. F. Xu, P. Li, X. Y. Wang, M. Xiao, Z. G. Zou, *Chem. Commun.*, 2015, **51**, 13354-13357.
28. Y. C. Zhou, X. X. Ran, A. Y. Chen, Y. Q. Chai, R. Yuan, Y. Zhuo, *Anal. Chem.* 2018, **90**, 9109-9116.
29. W. W. Tu, Y. T. Dong, J. P. Lei, H. X. Ju, *Anal. Chem.* 2010, **82**, 8711-8716.
30. B. C. Yin, Y. Q. Liu, B. C. Ye, *J. Am. Chem. Soc.* 2012, **134**, 5064-5067.
31. F. Degliangeli, P. Kshirsagar, V. Brunetti, P. P. Pompa, R. Fiammengo, *J. Am. Chem. Soc.* 2014, **136**, 2264-2267.